

# Trajectory Planning for the Five Degree of Freedom Feeding Robot Using Septic and Nonic Functions

Priyam A. Parikh

Mechanical Engineering Department, Nimra University, Ahmedabad, India

Email: 18ptphde189@nirmauni.ac.in

Reena Trivedi and Jatin Dave

Email: { reena.trivedi, jatin.dave }@nirmauni.ac.in

**Abstract**— In the present research work discusses about trajectory planning of five degrees of freedom serial manipulator using higher order polynomials. This robotic arm is used to feed semi-liquid food to the physically challenged people having fixed seating arrangement. It is essential to plan a smooth trajectory for proper delivery of food, without wasting it. Trajectory planning can be done in the joint space as well as in the cartesian space. It is difficult to design trajectory in Cartesian scheme due to non-existence of the Jacobian matrix. In the present research work, trajectory planning is done using joint space scheme. The joint space scheme offers lower and higher order polynomial methods for the trajectory planning. In the present work parabolic and cubic functions are considered as lower polynomials and septic (7<sup>th</sup> order) and nonic (9<sup>th</sup> order) functions are considered as higher order polynomials. Lower order polynomial does not have any control over joint acceleration and velocity, which leads a servo actuator towards instantaneous velocity and infinite acceleration. This phenomenon can cause loss of food in the delivery root, lesser battery life, wear and tear in the joints and increases the probability of damaging the servo actuator. To address this problem, the proposed research work presents the methodology and trajectory planning of a serial manipulator using septic and nonic functions. The higher order polynomials provide zero acceleration and velocity at the beginning and at the end. It also gives the continuity in the displacement, velocity and acceleration, which is necessary for smoother delivery of the food.

**Index Terms**—Feeding robot, trajectory planning, higher order polynomials, Lower order polynomials, septic function, nonic function, Physically challenged people.

## I. INTRODUCTION

Trajectory planning of a robot is to generate function according to which a robot's joint will move. Trajectory planning can be done using Cartesian scheme as well as joint space scheme [1]. However Cartesian scheme or inverse kinematics is essential to perform before getting into joint space scheme. Inverse kinematics mainly involves end-effector position, its orientation and derivatives.

Instead of planning the trajectory using Cartesian scheme, it is better to get the start point and end point of each joint [2]. After getting the joint angles from the operational space, trajectory planning can be done using joint space scheme. However trajectory planning in the Cartesian space allows accounting for the presence of any constraint along the path of the end-effector, but singular configuration and trajectory planning can't be done with operational space [3]. In the case of inverse kinematics no joint angle can be computed due to non-existence of the inverse of the Jacobian matrix. That is the reason behind selecting the joint space scheme for the trajectory planning [4].

Trajectory planning using joint space scheme can be done in many ways. General methods are linear function, parabolic function, cubic functions and quintic function. Above mentioned methods belong to lower order polynomial. This paper discusses about the trajectory planning using septic (7<sup>th</sup> order polynomials) and nonic (9<sup>th</sup> order polynomials). Lower orders polynomials are sometimes not desired due to its discontinuities in joint rates. Furthermore use of lower order polynomials in trajectory planning may lead robot to nonzero acceleration and velocity values at the beginning and at the end points of the trajectory. Sometimes use of first and second order polynomial may force servo actuator to provide instantaneous velocity and infinite acceleration, which leads servo motor towards locking or burning. Above mentioned conditions are not acceptable for this type of robot which carries food for patient.

Shuang Fang [5] has planned a trajectory using seventh order polynomial method. That method was applied on a seven degree of freedom robot. He got a smooth trajectory response compare to lower order polynomials, but he had not shown the problem of acceleration and velocity over shoots. Jiayan Zhang and Qingxi Meng [6] developed trajectory using improved genetic algorithm. Using this method they were able to reduce the cycle time of the robot as well as the trajectory got improved. Huang T. [7] applied the seventh-order B-spline curve for the trajectory planning, which achieved the optimal planning goal and the angular

displacement, velocity and acceleration curve of each joint of the robot are smoother. However spline curves are the combination of higher order and lower order polynomials to achieve the replica of the exact trajectory. Xiaojie Zhao and Maoli Wang [8] planned the robot trajectory using quintic polynomial method, which is nothing but a fifth order polynomial method. However this method could be useful when, initial and final angular velocities and angular acceleration are nonzero values.

The novelty of this research is; the robot trajectory is developed using seventh order and ninth order polynomials. In addition of angular displacement; angular velocity and acceleration are also given same the importance. The paper also discusses the merits and demerits of lower and higher order polynomials.

The first phase of the paper shows the basic details of robot, hardware set up, a 3D CAD model, forward and inverse kinematics. However forward and inverse kinematics are not necessary to show, but before discussing about the trajectories, velocity and acceleration, it becomes extremely important to discuss about forward and inverse kinematics. In addition with that forward kinematics gives information about the end-point of the robot (In this case end point is fixed). Based on this end-point in the Cartesian space, joint angles can be found (which is called inverse kinematics). The joint angles are found from inverse kinematics, can be rectified using joint space.

The second phase of the paper discusses about methodology of generating trajectories using septic and nonic functions. In addition with that, all the trajectories are compared and plotted along with velocity and acceleration.

A. Hardware Setup of the System

According to Fig. 1 (left), the robot is vertically downward and includes one twisting joint along with four revolute joints. The kinematic chain diagram is shown in Fig. 1 (right) along with the 3D model of the robot. In the kinematic chain diagram, the base and the spoon (end-effector) are denoted as B and G respectively. All the hardware details are shown in Table I.

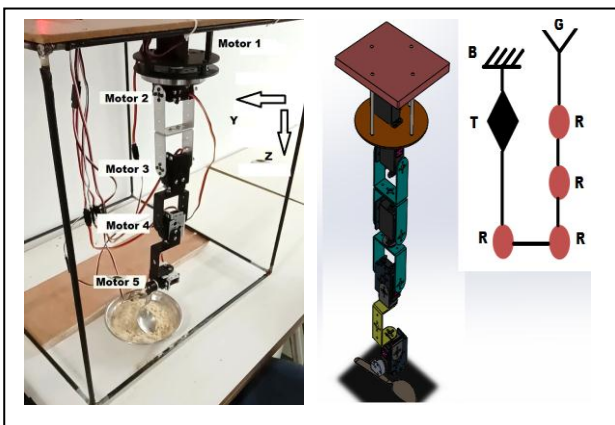


Figure 1. Hardware Setup and 3D CAD model along with kinetics diagram

TABLE I. HARDWARE DETAILS

Sr. No.	Details of Robot used in this paper	
	Particular	Details Remarks
1	Degree of Freedom	5
2	Type of Robot	T-R-R-R-R
3	Servo Motors X 5	Metal Gears, 15kg/cm torque (Stall torque)
4	Working Speed	0.13 sec/ 60 degree at 7.2 volts (No load)
5	Working Voltage	4.8 volt-7.2 volts
6	Controller Used	ARDUINO MEGA
7	Battery	LI-PO 7.2 volt
8	Sensor used	Gyroscope MPU6050 for Acceleration

B. Problem Description, Methodology and Work Flow

As discussed in the introduction part, lower order polynomial method does not provide any control over acceleration and velocity. However some researchers and text book authors has proposed a linear trajectory with parabolic blend, which is able to solve the problem of infinite acceleration. But this method contains linear trajectory, which makes angular acceleration almost zero and makes angular velocity maximum in the middle portion. So above mentioned method is also not desirable as far as the case of feeding robot is concerned. Then we tried to incorporate full cycloid trajectory based on cam and follower, but unfortunately it gave couple of acceleration and deceleration peaks. Next we replaced linear trajectory with exponential function. it worked well in the case of smoothness, but somehow, it got failed to provide zero acceleration and velocity at the end of the trajectory. At last we planned trajectory using seventh and ninth order polynomial methods. The purpose of zero acceleration and velocity at the beginning and end point of the trajectory is solved along with smother trajectory.

II. KINEMATIC MODELING USING DH MATRIX

Forward kinematics is for determining the position and orientation of a robot end-effector with respect to a reference coordinate system. In this case the joint variables and the arm parameters are already defined. Inverse kinematics of a robot manipulator deals with the calculation of each joint variable, given the position and orientation of end effector [9]. Forward kinematics is done using DH matrix frame assignment, where the methodology is explained to find end point of the end-effector using known  $\theta$  (Joint angle),  $\alpha$  (twisting angle),  $a$  (Link length) and  $d$  (joint distance).

A. Forward Kinematics Using DH Matrix Method

In (1), F is the function of  $\theta$ , by putting the value of  $\theta$ , values of desired position and rotation can be found [10]. Here  $\theta_1, \theta_2, \theta_3, \theta_4,$  and  $\theta_5$  are the input variables and  $x,y,z$  and  $R$  are the desired position and rotation respectively. The robot arm parameters are shown in Table II, which are generated using DH matrix frame assignment shown in Fig. 2.

$$F(\theta_1, \theta_2, \theta_3, \theta_4, \theta_5) = [x, y, z, R] \tag{1}$$

The forward kinematics assignment helps in finding the transformation of end-effector with respect to origin, which is shown in (2). Matrix shown in (3) is a transformation matrix, which is a combination of rotation matrix (3X3) and orientation (3X1) matrix. Equations 4 to 8 are derived by DH matrix frame assignment along with screw principle of rotation and translation. Equation 9 is a reference matrix to find all transformation matrices of the consecutive links.

Based on (9), all the transformation matrices are calculated for each joint. Referring Table II and putting all the initial values of each joint (column 1) in (9), we get the initial transformation matrix of the robot shown in (10).

Similarly putting all the final values of each joint in (column 2) (9), we get the final transformation matrix, shown in (11). It should be noted that  $(P_x, P_y, P_z)$  is the positional vector, whereas  $v_{11}$  to  $v_{33}$  is the rotational vector.

TABLE II. ROBOT ARM PARAMETERS (FORWARD KINEMATICS)

$\theta$ (Joint angle) Initial in Radian	$\theta$ (Joint angle) Final in Radian	d (joint distance )mm	$\alpha$ (twistin g angle) Radian	a (Link length) mm
$\theta_1=\pi$	$\theta_1=\pi$	50	$-\pi/2$	0
$\theta_2=\pi/2$	$\theta_1=2\pi/3$	0	0	140 (L1)
$\theta_3=0$	$\theta_1=2\pi/9$	0	0	120 (L2)
$\theta_4=0$	$\theta_1=\pi/9$	0	0	100(L3)
$\theta_5=-\pi/2$	$\theta_1=-\pi/18$	0	0	80(L4)

$${}^0T = {}^0T_1 {}^1T_2 {}^2T_3 {}^3T_4 {}^4T_5 \quad (2)$$

$${}^0T = \begin{bmatrix} v_{11} & v_{12} & v_{13} & P_x \\ v_{21} & v_{22} & v_{23} & P_y \\ v_{31} & v_{32} & v_{33} & P_z \\ 0 & 0 & 0 & 1 \end{bmatrix} \quad (3)$$

$${}^0T = \text{Rot}(\hat{Z}, \theta_1) \text{Rot}(\hat{X}, -90) \quad (4)$$

$${}^1T = \text{Rot}(\hat{Z}, \theta_2) \text{Trans}(\hat{X}, L_1) \quad (5)$$

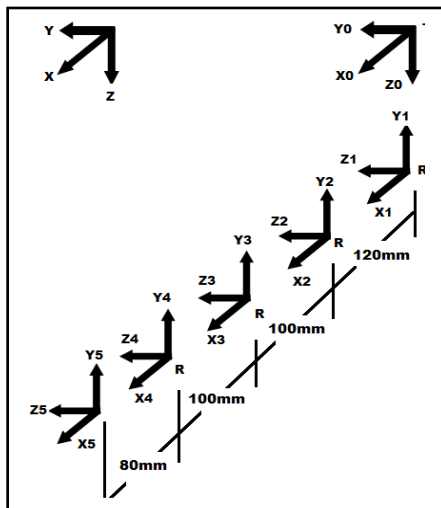


Figure 2. DH Matrix Frame Assignments on the current robotic system

$${}^2T = \text{Rot}(\hat{Z}, \theta_3) \text{Trans}(\hat{X}, L_2) \quad (6)$$

$${}^3T = \text{Rot}(\hat{Z}, \theta_4) \text{Trans}(\hat{X}, L_3) \quad (7)$$

$${}^4T = \text{Rot}(\hat{Z}, \theta_5) \text{Trans}(\hat{X}, L_4) \quad (8)$$

$${}^i-1T = \begin{bmatrix} C\theta_i & -S\theta_i C\alpha_i & S\theta_i S\alpha_i & a_i C\theta_i \\ S\theta_i & C\theta_i C\alpha_i & -C\theta_i S\alpha_i & a_i S\theta_i \\ 0 & S\alpha_i & C\alpha_i & d_i \\ 0 & 0 & 0 & 1 \end{bmatrix} \quad (9)$$

$${}^0T = \begin{bmatrix} -1 & 0 & 0 & -130 \\ 0 & 0 & -1 & 0 \\ 0 & -1 & 0 & -320 \\ 0 & 0 & 0 & 1 \end{bmatrix} \quad (10)$$

$${}^0T = \begin{bmatrix} 0.9848 & 0.1736 & 0 & 332.8 \\ 0 & 0 & -1 & 0 \\ -0.1736 & 0.9848 & 0 & -102 \\ 0 & 0 & 0 & 1 \end{bmatrix} \quad (11)$$

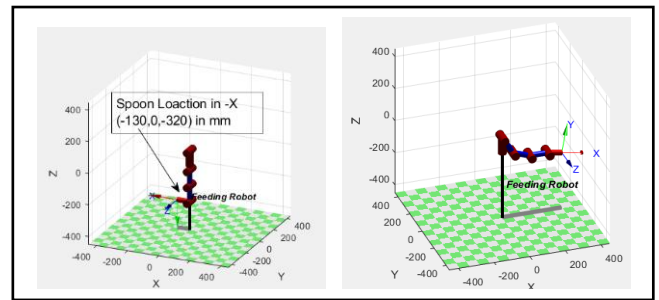


Figure 3. Initial and final position of the robot in XYZ plane before and after performing DH frame assignment

### B. Inverse Kinematics of the Robot

Inverse kinematics of a robot manipulator deals with the calculation of each joint variable, given the position and orientation of end effector. The computation of the inverse kinematics of robot manipulator is quite difficult if compared to the forward kinematics because of the nonlinearities and multiple solutions involved [12].

Inverse kinematics helps in finding modified joint angles, founded from forward kinematics. It should be noted that,  $C_{2345} = \cos(\theta_2 + \theta_3 + \theta_4 + \theta_5)$  and  $S_{234} = \sin(\theta_2 + \theta_3 + \theta_4)$ . Here the positional vector is the function of joint variables, shown in (12). The positional vectors can be given by (14) to (16) in XYZ plane. It can be found using the product of overall transformation matrix and inverse of first transformation matrix.

$$F(x, y, z, R) = [\theta_1, \theta_2, \theta_3, \theta_4, \theta_5] \quad (12)$$

$$[{}^0T]^{-1} {}^0T = {}^1T {}^2T {}^3T {}^4T {}^5T \quad (13)$$

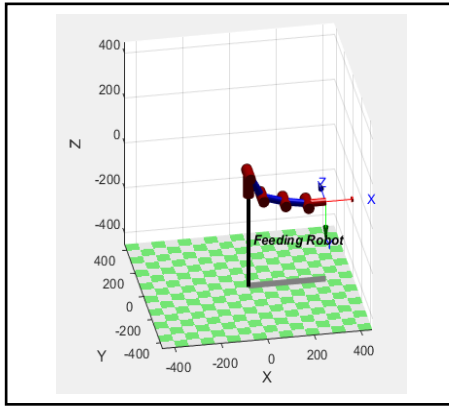


Figure 4. Final position of the robot in XYZ plane after inverse kinematics

$$P_x = C_1(L_1C_2 + L_2C_{23} + L_3C_{234} + L_4C_{2345}) \quad (14)$$

$$P_y = S_1(L_1C_2 + L_2C_{23} + L_3C_{234} + L_4C_{2345}) \quad (15)$$

$$P_z = 50 - (L_1S_2 - L_2S_{23} - L_3S_{234} - L_4S_{2345}) \quad (16)$$

After performing the inverse kinematics, the final position of the robot is shown in Fig. 4. All the joint angles, calculated using IK, are shown in Table III.

TABLE III. ROBOT INVERSE KINEMATIC ANALYSIS

Joints	$\theta_i$ (Joint angle) Initial in Radian	$\theta_f$ (Joint angle) Final in Radian	$\theta_i$ (Joint angle) Initial in Degree	$\theta_f$ (Joint angle) Final in Degree
Joint 1	$-12\pi/360$	$\pi/360$	-12.5	0
Joint 2	$120\pi/180$	$76\pi/180$	120	76
Joint 3	$\pi/360$	$-69\pi/180$	0	-69
Joint 4	$\pi/360$	$-6\pi/180$	0	-6
Joint 5	$-101\pi/180$	$\pi/360$	-101	0

### III. ROBOT TRAJECTORY PLANNING

As discussed earlier, robot trajectory planning is to ensure the smooth variation in the robotic joints. Trajectory planning also gives time history of position, velocity and acceleration at the intermediate point as well as final and starting point [13].

In the present case all the initial and final values of all the joints are known. Apart from that angular velocity at the beginning and at the end is kept zero [14].  $\theta$  is the angle in degree whereas  $t_i$  and  $t_f$  are the initial and final time respectively.  $\theta_i$  and  $\theta_f$  are the initial and final angles of the joints. All the angles are in degree and  $\theta_i, \dot{\theta}_i, \ddot{\theta}_i$  and  $\frac{d\dot{\theta}_i}{dt}$  are the initial angular displacement, angular velocity, angular acceleration, jerk and jounce respectively, whereas  $\theta_f, \dot{\theta}_f, \ddot{\theta}_f$  and  $\frac{d\dot{\theta}_f}{dt}$  are the final angular displacement, angular velocity, angular acceleration, jerk and jounce (4<sup>th</sup> time derivative) respectively [10].

#### A. Trajectory Planning Using 7<sup>th</sup> Order Polynomial

Angular displacement with respect to time with the order of seven is shown in (17). Since nth order polynomial would have n+ 1 coefficient, seventh order polynomial would have 8 coefficients. It's first, to fourth time derivatives are given in (18), (19) and (20) respectively. Here the first derivative represents angular velocity, second time derivative represents acceleration, whereas third and fourth derivative represents jerk and jounce respectively. All the initial and final conditions at time  $t=0$  seconds and  $t=t_f$  (final time) are shown in (21) to (24) respectively. All eight unknowns are found using  $AX=B$  (shown in 25). All the initial conditions, initial angles, final angles and all coefficients are shown in Table IV. In (27), the displacement function with respect to time is shown for all the joints. It should be noted that jounce is not discussed in this case. Eq. 26 to 31 represents all unknown coefficients. Eq. (31) represents generalized equation for displacement with all initial and final conditions. All the initial conditions for all the joints are shown in Table V. Coefficient values are shown in Table IV for septic function for all the joints.

$$\theta(t) = a + bt + ct^2 + dt^3 + et^4 + ft^5 + gt^6 + ht^7 \quad (17)$$

$$\dot{\theta}(t) = b + 2ct + 3dt^2 + 4et^3 + 5ft^4 + 6gt^5 + 7ht^6 \quad (18)$$

$$\ddot{\theta}(t) = 2c + 6dt + 12et^2 + 20ft^3 + 30gt^4 + 42ht^5 \quad (19)$$

$$\dddot{\theta}(t) = 6d + 24et + 60ft^2 + 120gt^3 + 210ht^4 \quad (20)$$

$$\theta(t) = \begin{cases} \theta_i = a, & t = 0 \text{ sec} \\ \theta_f = a + bt_f + ct_f^2 + dt_f^3 + et_f^4 + ft_f^5 + gt_f^6 + ht_f^7, & t = t_f \text{ sec} \end{cases} \quad (21)$$

$$\dot{\theta}(t) = \begin{cases} \dot{\theta}_i = b, & t = 0 \text{ sec} \\ \dot{\theta}_f = b + 2ct_f + 3dt_f^2 + 4et_f^3 + 5ft_f^4 + 6gt_f^5 + 7ht_f^6, & t = t_f \text{ sec} \end{cases} \quad (22)$$

$$\ddot{\theta}(t) = \begin{cases} \ddot{\theta}_i = 2c, & t = 0 \text{ sec} \\ \ddot{\theta}_f = 2c + 6dt_f + 12et_f^2 + 20ft_f^3 + 30gt_f^4 + 42ht_f^5, & t = t_f \text{ sec} \end{cases} \quad (23)$$

$$\dddot{\theta}(t) = \begin{cases} \dddot{\theta}_i = 6d, & t = 0 \text{ sec} \\ \dddot{\theta}_f = 6d + 24et_f + 60ft_f^2 + 120gt_f^3 + 210ht_f^4, & t = t_f \text{ sec} \end{cases} \quad (24)$$

$$\begin{bmatrix} 1 & 0 & 0 & 0 & 0 & 0 & 0 & 0 \\ 1 & t_f & t_f^2 & t_f^3 & t_f^4 & t_f^5 & t_f^6 & t_f^7 \\ 0 & 1 & 0 & 0 & 0 & 0 & 0 & 0 \\ 0 & 1 & 2t_f & 3t_f^2 & 4t_f^3 & 5t_f^4 & 6t_f^5 & 7t_f^6 \\ 0 & 0 & 2 & 0 & 0 & 0 & 0 & 0 \\ 0 & 0 & 2 & 6t_f & 12t_f^2 & 20t_f^3 & 30t_f^4 & 42t_f^5 \\ 0 & 0 & 0 & 6 & 0 & 0 & 0 & 0 \\ 0 & 0 & 0 & 6 & 24t_f & 60t_f^2 & 120t_f^3 & 210t_f^4 \end{bmatrix} \begin{bmatrix} a \\ b \\ c \\ d \\ e \\ f \\ g \\ h \end{bmatrix} = \begin{bmatrix} \theta_i \\ \theta_f \\ \dot{\theta}_i \\ \dot{\theta}_f \\ \ddot{\theta}_i \\ \ddot{\theta}_f \\ \ddot{\theta}_i \\ \ddot{\theta}_f \end{bmatrix} \quad (25)$$

$$a = \theta_i, b = \dot{\theta}_i, c = \ddot{\theta}_i/2, d = \dddot{\theta}_i/6 \quad (26)$$

$$e = 35 \frac{(\theta_f - \theta_i)}{t_f^4} - \frac{5}{t_f^3} (3\dot{\theta}_f + 4\dot{\theta}_i) + 5 \frac{(0.5\ddot{\theta}_f - \ddot{\theta}_i)}{t_f^2} - \frac{\ddot{\theta}_i}{6t_f} \quad (27)$$

$$f = 84 \frac{(\theta_i - \theta_f)}{t_f^5} + \frac{1}{t_f^4} (39\theta_f + 45\theta_i) + \frac{(10\ddot{\theta}_i - 7\ddot{\theta}_f)}{t_f^3} + \frac{\ddot{\theta}_i + 0.5\ddot{\theta}_f}{2t_f^2} \quad (28)$$

$$g = 70 \frac{(\theta_f - \theta_i)}{t_f^6} - \frac{1}{t_f^5} (34\theta_f + 36\theta_i) + \frac{(13\ddot{\theta}_f - 15\ddot{\theta}_i)}{2t_f^4} - \frac{2\ddot{\theta}_i}{3t_f^3} - \frac{\ddot{\theta}_f}{2t_f^2} \quad (29)$$

$$h = 20 \frac{(\theta_i - \theta_f)}{t_f^7} + \frac{10}{t_f^6} (\dot{\theta}_f + \dot{\theta}_i) + 2 \frac{(\ddot{\theta}_i - \ddot{\theta}_f)}{t_f^5} + \frac{(\ddot{\theta}_i + \ddot{\theta}_f)}{6t_f^4} \quad (30)$$

$$\theta(t) = \theta_i + 35 \frac{(\theta_f - \theta_i)}{t_f^4} t^4 + 84 \frac{(\theta_i - \theta_f)}{t_f^5} t^5 + 70 \frac{(\theta_f - \theta_i)}{t_f^6} t^6 + 20 \frac{(\theta_i - \theta_f)}{t_f^7} t^7 \quad (31)$$

$$\theta(t) = \begin{cases} -12.5 - 0.33t^4 + 0.13t^5 - 0.018t^6 + 0.0009t^7, & \text{For joint 1} \\ 120 - 0.03t^4 + 0.47t^5 - 0.066t^6 + 0.003t^7, & \text{For joint 2} \\ -1.86t^4 + 0.74t^5 - 0.10t^6 + 0.005t^7, & \text{For joint 3} \\ -0.16t^4 + 0.06t^5 - 0.009t^6 + 0.0004t^7, & \text{For joint 4} \\ -101 + 2.72t^4 - 1.09t^5 + 0.15t^6 - 0.0072t^7, & \text{For joint 5} \end{cases} \quad (32)$$

TABLE IV. COEFFICIENTS VALUES FOR SEPTIC FUNCTION

Coefficients and Initial Conditions	Joint 1	Joint 2	Joint 3	Joint 4	Joint 5
a	-12.5	120	0.5	0.5	-101
b	0	0	0	0	0
c	0	0	0	0	0
d	0	0	0	0	0
e	-0.33	-0.03	-1.86	-0.16	2.72
f	0.13	0.47	0.74	0.06	-1.09
g	-0.018	-0.066	-0.1	-0.009	0.15
h	$\frac{0.0000}{9}$	0.003	0.005	0.0004	-0.0072
$\theta_i$	-12.5	120	0.5	0.5	-101
$\theta_f$	0.5	76	-69	-6	0.5

TABLE V. INITIAL CODITIONS FOR ALL THE JOINTS

	Joint 1	Joint 2	Joint 3	Joint 4	Joint 5
$\dot{\theta}(t)$	0	0	0	0	0
$\theta(t)$	0	0	0	0	0
$\theta''(t)$	0	0	0	0	0
$\frac{d}{dt}\theta''(t)$	0	0	0	0	0

**B. Trajectory Planning Using 9<sup>th</sup> Order Polynomial**

Angular displacement with respect to time with the order of seven is shown in (33). It's first, to fourth time derivatives are given in (34) to (37) respectively. Here the first derivative represents angular velocity, second time

derivative represents acceleration, whereas third and fourth derivative represents jerk and jounce respectively. All the initial and final conditions at time t=0 seconds and t=t<sub>f</sub> (final time) are shown in (38) to (42) respectively. All eight unknowns are found using AX=B (shown in 43). All the initial conditions, initial angles, final angles and all coefficients are shown in Table V. In (27), the displacement function with respect to time is shown for all the joints. Eq. 44 to 49 represents all unknown coefficients. Eq. (50) represents generalized equation for displacement with all initial and final conditions. Coefficient values are shown in Table VI for nonic function for all the joints.

$$\theta(t) = a + bt + ct^2 + dt^3 + et^4 + ft^5 + gt^6 + ht^7 + it^8 + jt^9 \quad (33)$$

$$\dot{\theta}(t) = b + 2ct + 3dt^2 + 4et^3 + 5ft^4 + 6gt^5 + 7ht^6 + 8it^7 + 9jt^8 \quad (34)$$

$$\theta''(t) = 2c + 6dt + 12et^2 + 20ft^3 + 30gt^4 + 42ht^5 + 56it^6 + 72jt^7 \quad (35)$$

$$\theta'''(t) = 6d + 24et + 60ft^2 + 120gt^3 + 210ht^4 + 336it^5 + 504jt^6 \quad (36)$$

$$\frac{d}{dt}\theta'''(t) = 24e + 120ft + 360gt^2 + 840ht^3 + 1680it^4 + 3024jt^5 \quad (37)$$

$$\theta(t) = \begin{cases} \theta_i = a, & t = 0 \text{ sec} \\ \theta_f = a + bt_f + ct_f^2 + dt_f^3 + et_f^4 + ft_f^5 + gt_f^6 + ht_f^7 + it_f^8 + jt_f^9 & t = t_f \end{cases} \quad (38)$$

$$\dot{\theta}(t) = \begin{cases} \dot{\theta}_i = b, & t = 0 \text{ sec} \\ \dot{\theta}_f = b + 2ct_f + 3dt_f^2 + 4et_f^3 + 5ft_f^4 + 6gt_f^5 + 7ht_f^6 + 8it_f^7 + 9jt_f^8, & t_f \text{ sec} \end{cases} \quad (39)$$

$$\theta''(t) = \begin{cases} \theta''_i = 2c & t = 0 \text{ sec} \\ \theta''_f = 2c + 6dt_f + 12et_f^2 + 20ft_f^3 + 30gt_f^4 + 42ht_f^5 + 56it_f^6 + 72jt_f^7 & \text{at } t = t_f \text{ sec} \end{cases} \quad (40)$$

$$\theta'''(t) = \begin{cases} \theta'''_i = 6d & t = 0 \text{ sec} \\ \theta'''_f = 6d + 24et_f + 60ft_f^2 + 120gt_f^3 + 210ht_f^4 + 336it_f^5 + 504jt_f^6, & \text{at } t = t_f \end{cases} \quad (41)$$

$$\frac{d}{dt}\theta''(t) = \begin{cases} \frac{d}{dt}\ddot{\theta}_i = 24e, \text{ at } t = 0 \text{ sec} \\ \frac{d}{dt}\ddot{\theta}_f = 6d + 24et_f + 60ft_f^2 + 120gt_f^3 + 210ht_f^4 + 336it_f^5 + 504jt_f^6 \\ \text{ at } t = t_f \text{ sec} \end{cases} \quad (42)$$

$$\begin{bmatrix} 1 & 0 & 0 & 0 & 0 & 0 & 0 & 0 & 0 & 0 \\ 1 & t_f & t_f^2 & t_f^3 & t_f^4 & t_f^5 & t_f^6 & t_f^7 & t_f^8 & t_f^9 \\ 0 & 1 & 0 & 0 & 0 & 0 & 0 & 0 & 0 & 0 \\ 0 & 1 & 2t_f & 3t_f^2 & 4t_f^3 & 5t_f^4 & 6t_f^5 & 7t_f^6 & 8t_f^7 & 9t_f^8 \\ 0 & 0 & 2 & 0 & 0 & 0 & 0 & 0 & 0 & 0 \\ 0 & 0 & 2 & 6t_f & 12t_f^2 & 20t_f^3 & 30t_f^4 & 42t_f^5 & 56t_f^6 & 72t_f^7 \\ 0 & 0 & 0 & 6 & 0 & 0 & 0 & 0 & 0 & 0 \\ 0 & 0 & 0 & 0 & 24t_f & 60t_f^2 & 120t_f^3 & 210t_f^4 & 336t_f^5 & 504t_f^6 \\ 0 & 0 & 0 & 0 & 24 & 0 & 0 & 0 & 0 & 0 \\ 0 & 0 & 0 & 0 & 24 & 120t_f & 360t_f^2 & 840t_f^3 & 1680t_f^4 & 3024t_f^5 \end{bmatrix} \begin{bmatrix} a \\ b \\ c \\ d \\ e \\ f \\ g \\ h \\ i \\ j \end{bmatrix} = \begin{bmatrix} \theta_i \\ \dot{\theta}_i \\ \ddot{\theta}_i \\ \dot{\theta}_f \\ \ddot{\theta}_f \\ \frac{d}{dt}\ddot{\theta}_i \\ \frac{d}{dt}\ddot{\theta}_f \end{bmatrix} \quad (43)$$

$$a = \theta_i \quad b = \dot{\theta}_i \quad c = \frac{\ddot{\theta}_i}{2} \quad d = \frac{\ddot{\theta}_i}{6} \quad e = \frac{d}{dt}\left(\frac{\ddot{\theta}_i}{24}\right) \quad (44)$$

$$f = 126 \frac{(\theta_f - \theta_i)}{t_f^5} - \frac{(56\ddot{\theta}_f + 70\dot{\theta}_i)}{t_f^4} + \frac{(21\ddot{\theta}_i - 35\ddot{\theta}_f)}{2t_f^3} - \frac{(\dot{\theta}_f + 2.5\dot{\theta}_i)}{t_f^2} + \frac{d}{dt}\left(\frac{\ddot{\theta}_f}{t_f}\right) \quad (45)$$

$$g = 420 \frac{(\theta_f - \theta_i)}{t_f^6} + 4 \frac{(49\dot{\theta}_f + 61\dot{\theta}_i)}{t_f^5} + \frac{(105\ddot{\theta}_i - 77\ddot{\theta}_f)}{2t_f^4} + \frac{(20\ddot{\theta}_i + 11.5\ddot{\theta}_f)}{3t_f^3} + \frac{2.5 \frac{d}{dt}\ddot{\theta}_i - \frac{d}{dt}\ddot{\theta}_f}{6t_f^2} \quad (46)$$

$$h = 540 \frac{(\theta_f - \theta_i)}{t_f^7} - 20 \frac{(13\dot{\theta}_f + 14\dot{\theta}_i)}{t_f^6} + \frac{(53\ddot{\theta}_f - 63\ddot{\theta}_i)}{t_f^5} - \frac{(15\dot{\theta}_i + 11\ddot{\theta}_f)}{2t_f^4} + \frac{d}{dt}\ddot{\theta}_f - \frac{5 \frac{d}{dt}\ddot{\theta}_i}{4t_f^3} \quad (47)$$

$$i = 315 \frac{(\theta_f - \theta_i)}{t_f^8} + 5 \frac{(\dot{\theta}_f - 40\dot{\theta}_i)}{t_f^7} + 5 \frac{(7\ddot{\theta}_i - 7.5\ddot{\theta}_f)}{t_f^6} + \frac{(2\ddot{\theta}_i + 7\ddot{\theta}_f)}{2t_f^5} - \frac{d}{dt}\ddot{\theta}_f - \frac{5 \frac{d}{dt}\ddot{\theta}_i}{6t_f^4} \quad (48)$$

$$j = 70 \frac{(\theta_f - \theta_i)}{t_f^9} - 35 \frac{(\dot{\theta}_f + \dot{\theta}_i)}{t_f^8} + 7.5 \frac{(\ddot{\theta}_f - \ddot{\theta}_i)}{t_f^7} - 5 \frac{(\ddot{\theta}_i + \ddot{\theta}_f)}{6t_f^6} - \frac{d}{dt}\ddot{\theta}_f - \frac{d}{dt}\ddot{\theta}_i \quad (49)$$

$$\theta(t) = \theta_i + 126 \frac{(\theta_f - \theta_i)}{t_f^5} t^5 + 420 \frac{(\theta_f - \theta_i)}{t_f^6} t^6 + 540 \frac{(\theta_f - \theta_i)}{t_f^7} t^7 + 315 \frac{(\theta_f - \theta_i)}{t_f^8} t^8 + 70 \frac{(\theta_f - \theta_i)}{t_f^9} t^9 \quad (50)$$

$$\theta(t) = \begin{cases} -12.5 + 0.20t^5 - 0.11t^6 + 0.024t^7 - 0.0023t^8 + 0.00008t^9, & \text{For J1} \\ 120 - 0.71t^5 + 0.39t^6 - 0.084t^7 + 0.0082t^8 + 0.00008t^9, & \text{For J2} \\ 0.20t^5 - 0.11t^6 + 0.024t^7 - 0.0023t^8 - 0.0005t^9, & \text{For J3} \\ -0.1t^5 + 0.054t^6 - 0.011t^7 + 0.0011t^8 - 0.00004t^9, & \text{For J4} \\ -101 + 1.63t^5 - 0.91t^6 + 0.19t^7 - 0.019t^8 + 0.0007t^9, & \text{For J5} \end{cases} \quad (51)$$

TABLE VI. COEFFICIENTS VALUES FOR NONIC FUNCTION

Coefficients and Initial Conditions	Joint 1	Joint 2	Joint 3	Joint 4	Joint 5
<i>a</i>	-12.5	120	0.5	0.5	-101
<i>b</i>	0	0	0	0	0
<i>c</i>	0	0	0	0	0
<i>d</i>	0	0	0	0	0
<i>e</i>	0	0	0	0	0
<i>f</i>	0.2	-0.71	0.20	-0.1	1.63
<i>g</i>	-0.11	0.39	-0.11	0.054	-0.91
<i>h</i>	0.024	-0.084	0.024	-0.011	0.19
<i>i</i>	-0.0023	0.0082	-0.0023	0.0011	-0.019
<i>j</i>	0.00008	0.00008	-0.0005	-0.00004	0.0007
$\theta_i$	-12.5	120	0.5	0.5	-101
$\theta_f$	0.5	76	-69	-6	0.5

IV. RESULTS AND DISCUSSION

TABLE VII. VALUES OF VELOCITY AND ACCELERATION AT THE INITIAL, MIDDLE AND FINAL POINT OF THE TRAJECTORY

Order of Function		0 sec	3 sec	6 sec
Parabolic	Velocity In deg/sec	0	17	33
	Acc In Deg/sec^2	5.5	5.5	5.5
Cubic	Velocity	0	25	0
	Acc	18	0	-17
Septic	Velocity	0	37	0
	Acc	0	0	0
Nonic	Velocity	0	41	0
	Acc	0	0	0

Table VI shows the values of velocity and acceleration at the beginning, middle and end of the trajectory. Angular displacement, velocity and acceleration are compared and plotted in fig 5 to 7 respectively. However methodology for parabolic function and cubic function are not shown in this paper. Based on these plots, values of velocity and acceleration are mentioned in Table VI. Trajectory design using second order or parabolic function provides zero velocity at the beginning, but fails to provide zero velocity at the end. It also provides constant acceleration through the entire trajectory. Cubic polynomial is able to satisfy zero velocity at the ends, but fails to give zero acceleration for the same. Meanwhile higher order polynomials are able to satisfy zero velocity and acceleration at the ends. However higher order functions leave over shoot acceleration and velocity at the middle of the trajectory.

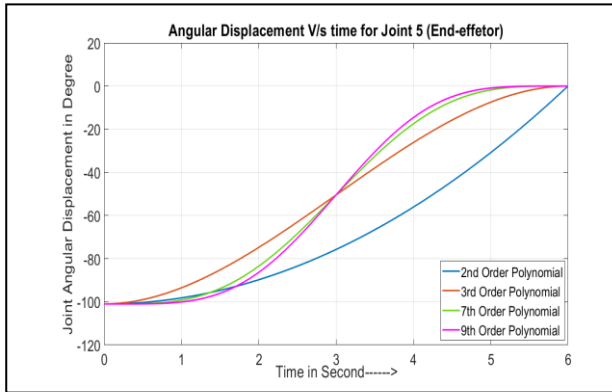


Figure 5. Angular displacement comparison for Joint 5

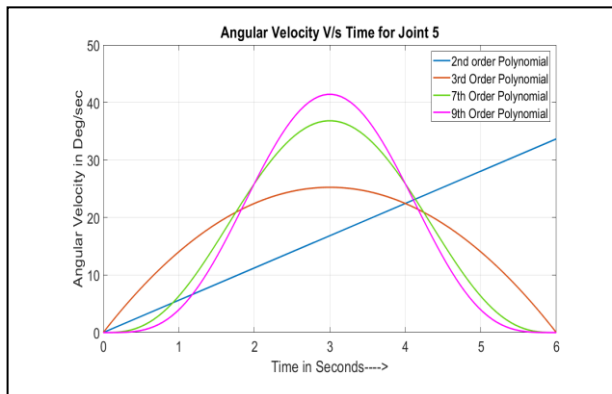


Figure 6. Angular velocity comparison of Joint 5

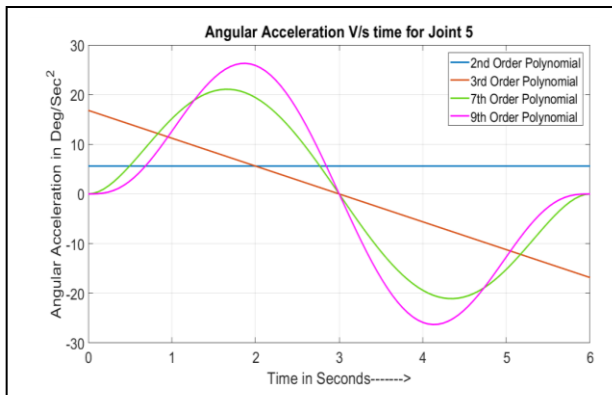


Figure 7. Angular acceleration comparison of Joint 5

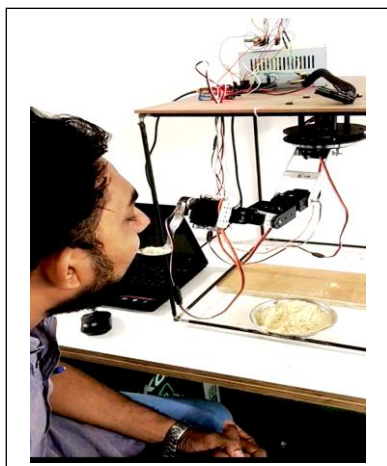


Figure 8. Final Position of the Robot in XZ plane after applying 7<sup>th</sup> order polynomial method (real time)

## V. CONCLUSIONS

From the work presented in this paper, it is concluded that the trajectory planning using septic and nonic functions is successfully deployed for maintaining the continuity of joint velocity and acceleration. It also satisfies zero velocity and acceleration at the ends of the trajectory. Septic and nonic functions give smoother trajectory compare to parabolic and cubic polynomials, which helps robot in delivering the food without wasting it. It also increases the battery life and life of a servo actuator due to its continuous response of velocity and acceleration. The limitation of the paper is that, higher order polynomials provide peaks of acceleration and velocity in the middle of the trajectory, which is not desired for multiple point trajectory. In the future, trajectory planning can be done using optimization algorithms like PSO, GA and ANN. Also fuzzy PID based dynamic control system can be designed to have a more control over joint angles, velocity and acceleration.

## CONFLICT OF INTEREST

The authors declare no conflict of interest in this research.

## AUTHOR CONTRIBUTIONS

Please state each author's contribution to this work. Priyam Parikh did the trajectory planning using lower and higher order polynomials. He also developed the entire robotic arm along with programming in MATLAB and ARDUINO. Co-author Dr. Reena Trivedi did the motion planning, simulation and 3D modeling. Dr. Jatin Dave helped in calculating forward and inverse kinematics of the serial manipulator.

## REFERENCES

- [1] A. Valente, S. Baraldo, and E. Carpanzano, "Smooth trajectory generation for industrial robots performing high precision assembly processes," *CIRP Annals*, vol. 66, no. 1, pp. 17–20, 2017.
- [2] A. Gasparetto and V. Zanutto, "Optimal trajectory planning for industrial robots," *Advances in Engineering Software*, vol. 41, no. 4, pp. 548–556, 2010.
- [3] W. G. Hao, Y. Y. Leck, L. C. Hun, "6-DOF PC-Based Robotic Arm (PC-ROBOARM) with efficient trajectory planning and speed control," in *Proc. 2011 4th International Conference on Mechatronics (ICOM)*, 2011.
- [4] F. Basile, F. Caccavale, P. Chiacchio, J. Coppola, C. Curatella, "Task-oriented motion planning for multi-arm robotic systems," *Robotics and Computer-Integrated Manufacturing*, vol. 28, no. 5, pp. 569–582, 2012.
- [5] S. Fang, X. Ma, J. Qu, S. Zhang, N. Lu, X. Zhao, "Trajectory planning for seven-DOF robotic arm based on seventh degree polynomial," in: Jia Y., Du J., Zhang W. (eds) *Proceedings of 2019 Chinese Intelligent Systems Conference. CISC 2019. Lecture Notes in Electrical Engineering*, vol. 593. Springer, Singapore, 2020.
- [6] J. Zhang, Q. Meng, X. Feng, H. Shen, "A 6-DOF robot-time optimal trajectory planning based on an improved genetic algorithm," *Robotics and Biomimetics*, vol. 5, no. 1, 2018
- [7] Y. Li, T. Huang, D. G. Chetwynd, "An approach for smooth trajectory planning of high-speed pick-and-place parallel robots using quintic B-splines," *Mechanism and Machine Theory*, vol. 126, pp. 479–490.

- [8] X. J. Zhao, M. L. Wang, N. Liu, and Y. W. Tang, "Trajectory planning for 6-DOF robotic arm based on quintic polynomial," in *Proc. the 2017 2nd International Conference on Control, Automation and Artificial Intelligence (CAAI 2017)*, [Online]. Available: <https://doi.org/10.2991/caai-17.2017.23>
- [9] J. Rosell, A. Perez, A. Aliakbar, Muhayyuddin, L. Palomo, and N. Garcia, "The Kautham project: A teaching and research tool for robot motion planning," in *Proc. the 2014 IEEE Emerging Technology and Factory Automation (ETFA)*, 2014.
- [10] J. M. Longval, C. Gosselin, "Dynamic trajectory planning and geometric design of a two-DOF translational cable-suspended planar parallel robot using a parallelogram cable loop," vol. 5B, 42nd Mechanisms and Robotics Conference, 2018.
- [11] X. Jiang, E. Barnett, and C. Gosselin, "Dynamic point-to-point trajectory planning beyond the static workspace for six-DOF cable-suspended parallel robots," *IEEE Transactions on Robotics*, vol. 34, no. 3, pp. 781–793, 2018.
- [12] X. Wang, D. Zhang, C. Zhao, H. Zhang, and H. Yan, "Singularity analysis and treatment for a 7R 6-DOF painting robot with non-spherical wrist," *Mechanism and Machine Theory*, vol. 126, pp. 92–107, 2018.
- [13] M. Vulliez, S. Zeghloul, and O. Khatib, "Kinematic analysis of the delthaptic, a new 6-DOF haptic device," *Springer Proceedings in Advanced Robotics*, pp. 181–189, 2017.
- [14] S. Zhu, Wang, "Time-optimal and jerk-continuous trajectory planning algorithm for manipulators," *J Mech Eng.*, 2010;46(3):456–62. [Online]. Available: <https://doi.org/10.3901/jme.20>.

Copyright © 2020 by the authors. This is an open access article distributed under the Creative Commons Attribution License ([CC BY-NC-ND 4.0](https://creativecommons.org/licenses/by-nc-nd/4.0/)), which permits use, distribution and reproduction in any medium, provided that the article is properly cited, the use is non-commercial and no modifications or adaptations are made.



**Priyam Parikh** is currently pursuing his PhD in mechanical engineering from Nirma University, Gujarat, India. He is also working as an Assistant Professor at Anant National University in Industrial Design Department. He has done his masters in Mechatronics Engineering from G.H. Patel College of Engineering and technology, VVnagar, India. His area of interest is Robotics, Automation, Mechatronics and Industrial Design.